An Acad Bras Cienc (2022) 94(Suppl. 1): e20210482 DOI 10.1590/0001-3765202220210482
Anais da Academia Brasileira de Ciências | *Annals of the Brazilian Academy of Sciences*
Printed ISSN 0001-3765 I Online ISSN 1678-2690
www.scielo.br/aabc | www.fb.com/aabcjournal

GEOSCIENCES

Geomorphology of Martel inlet, King George Island, Antarctica: a new interpretation based on multi-resolution topo-bathymetric data

CLEIVA PERONDI, KÁTIA KELLEM DA ROSA, ROSEMARY VIEIRA, FABIO JOSÉ G. MAGRANI, ARTHUR AYRES NETO & JEFFERSON C. SIMÕES

Abstract: This study investigated the terrestrial and submarine geomorphology and glacial landform records in the Martel inlet (King George Island) using a multi-resolution topobathymetric data based on seismic, multibeam surveys and terrestrial satellite datasets (REMA DEM). Geomorphometric analysis provided glacial landforms and sedimentary processes interpretation. The submarine sector has a mean depth of 143 m, a maximum depth of 398 m, and most of it has a low slope (0°–16°). Steep slopes (>30°) are found along the mid-outer sectors transition area. The continental shelf was divided into inner fjord (49 m depth), middle fjord (119 m), and outer fjord (259 m), based on depth, elevation and slope. The topobathymetric digital model provides evidence of geomorphological contrasts between these zones in the fjord's seafloor and subaerial environments. A prominent morainal bank in the transition between the inner and middle parts marks the limit of a past stationary stage of the Dobrowolski-Goetel ice margin. Streamlined glacial lineations demonstrate an NE-SW past ice flow direction and a wet-based thermal regime. The combined analysis of submarine and subaerial landforms enable the understanding of the former glacier configuration and its deglaciation history.

Key words: Antarctic fjord, submarine landform, multibeam bathymetry, glacier forelands, palaeoglacial history.

INTRODUCTION

Fjords are generally deep and coastal areas, mostly located at medium and high latitudes (Benn & Evans 2010). The characteristic morphology of fjords is the product of erosion by outlet glaciers over multiple late Cenozoic glacial cycles (Dyer 1997, Bianchi et al. 2020) and sea-level fluctuations since the Last Glacial Maximum (LGM) (Syvitski et al. 1987). Tectonic structures, including faults, pre-existing fractures, and intrusions influence the formation of fjords and govern the alignment of the ice flow (Glasser & Ghiglione 2009, Benn & Evans 2010).

Fjord sedimentary processes and deposits reflect ice-contact, proximal, distal, and paraglacial (subaerial) depositional environments (Syvitski 1993). Therefore, their glacimarine environments are governed by processes linked to glaciers, oceans, and the biosphere that transport, deposit, and rework their sediments (Dowdeswell & Scourse 1990).

In glacimarine environments, glacimarine landforms are produced at either the margins of a grounded tidewater glacier or at the grounding zone of floating ice shelves (Powell 1984, Dowdeswell et al. 2016). Fluctuations in these tidewater terminus positions are governed by the balance between ice velocity, ice calving,

bedrock instabilities, atmospheric dynamics, and frontal ablation rates (Otero et al. 2017, Bianchi et al. 2020). Thus, controlling factors such as fjord bathymetry and topography exert a strong influence on the response of tidewater glaciers to climate change (Bianchi et al. 2020).

Located at King George Island (KGI), Admiralty Bay (AB) is an example of a fjord-system, with an area of 122 km² (Siciński et al. 2011). Martel Inlet (MI) is a semi-closed fjord inside AB that is aligned to the SW. The area is characterized today by the presence of relatively small, highly crevassed tidewater glaciers (Ajax, Stenhouse, Goetel, Dobrowolski, and Krak) with steep slopes. Some glaciers are land terminating, including Wanda, Dragon, and Professor. The glacierized area in MI has undergone recent changes and lost about 6.64 km² of its ice mass (13.2% of the total area) since 1979 (Rosa et al. 2013).

During the LGM, glaciers reached the Bransfield Strait and filled the fjords (John & Sugden 1971). Since the LGM, the South Shetland Islands (SSI) have experienced progressive postglacial warming, with a few minor cooling events associated with glacier advances (Hall 2007). Various stages of deglaciation in KGI have been suggested from the early to middle Holocene (Mausbacher 1991). Terrestrial evidence in the SSI suggests mild and humid climatic conditions peaking between 3.0 and 2.8 cal ka BP (Björck et al. 1993). Between 4.5 and 2.8 ka BP tidewater glaciers on the KGI retreated from the tributary fjords in Maxwell Bay (Yoon et al. 2000), although ice may have persisted in small coves until 1.7 cal ka BP (Simms et al. 2011). At the AB margin, studies suggest deglaciation of the shallow marine platform around 1.9 and 1.2 cal ka BP (Yoon et al. 2000, Simms et al. 2011). Some Late Holocene marine and terrestrial records from the SSI (Fabrés et al. 2000) indicate warmer temperatures between 1.4 and 0.55 cal ka BP and a cooler period at 0.55 and 0.05 cal ka BP (Fabrés et al. 2000). Radiocarbon dates from moraines indicate an advance of the Collins Ice Cap on the Fildes Peninsula (King George Island) after ~650 cal a BP (~AD 1300). This advance is the most extensive of the last 3,500 cal (Hall, 2007).

Magrani et al. (2015) showed a variable and irregular bottom morphology of AB and the submarine landforms observed in the modern setting of MI and AB. The submarine and terrestrial landforms oriented transverse to the direction of ice flow to reveal long-term changes in glacier terminus position (Dowdeswell et al. 2016, Chandler et al. 2016).

This study investigated the terrestrial and submarine geomorphological records of Martel Inlet based on multi-resolution topobathymetric data. The MI geomorphology, physiography and topography characterization reveals the different depositional sectors of Martel Inlet, and their linkages and contrasting's. The goals of this study are to characterize the paleo-ice flow (past ice flow direction and a basal-thermal regime) and to provide some evidence for the recent and long-term glacial changes in the region.

STUDY AREA AND ENVIRONMENTAL SETTING

The Martel Inlet (62°06'S, 58° 20'W) (Figure 1), located at Admiralty Bay, King George Island (KGI), South Shetland Islands (SSI), northern Antarctic Peninsula region (Figure 1A), is an area of special interest for the Brazilian Antarctic Program (PROANTAR).

MI is linked to the Ezcurra fault (Figure 1C) system (NE-SW), Barton Horst, and Warszawa tectonic blocks (Birkenmajer 1991). A new system of transverse faults, including the Kraków Fault (N-S), formed at approximately 54 Ma and remained active until 21 Ma due to movements

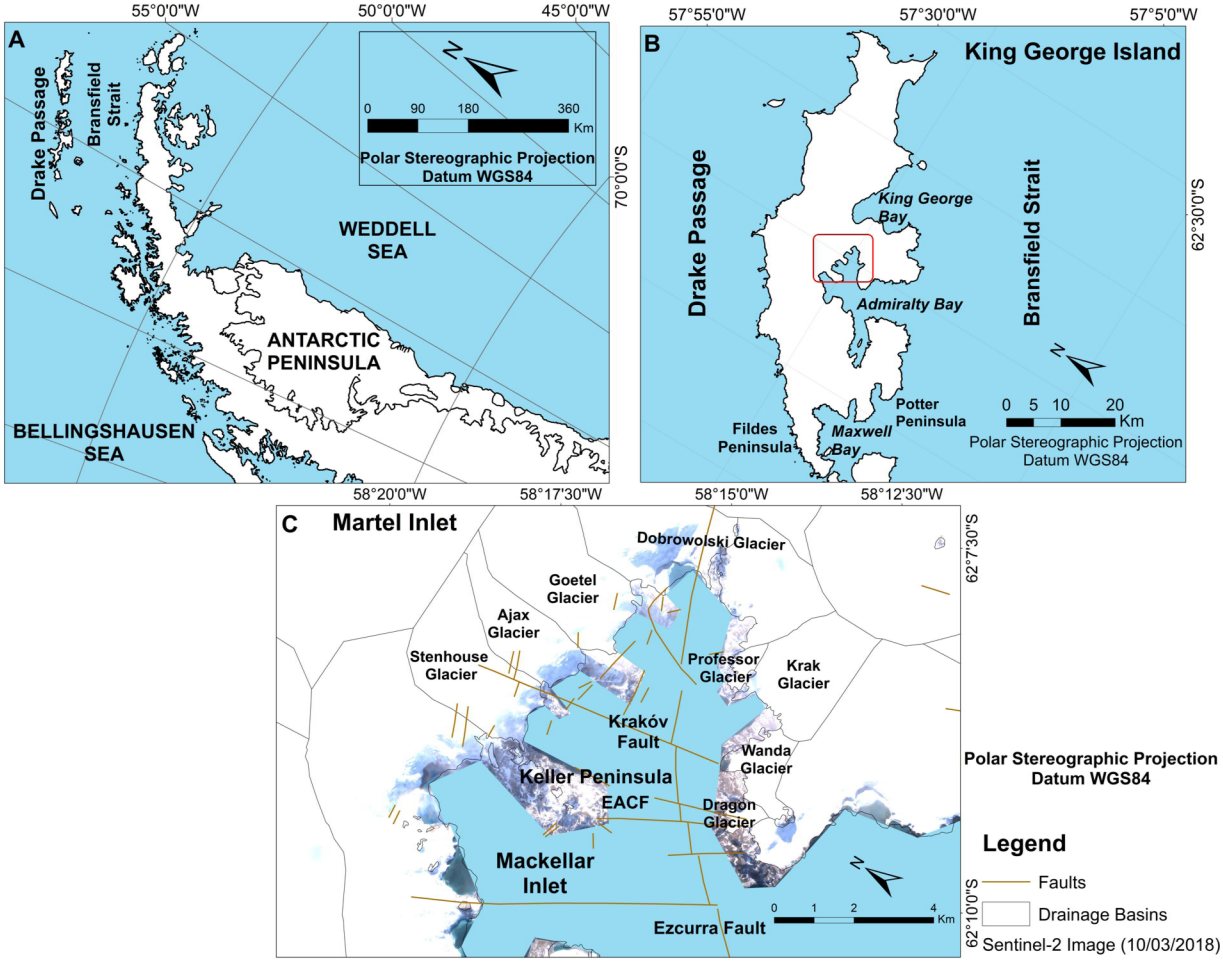

Figure 1. Location map. a) KGI location northeast of the Antarctic Peninsula. b) Location of Martel Inlet (MI) on King George Island. c) MI and the current glaciers. Comandante Ferraz Antarctic Station (EACF). Data source: Quantarctica (Matsuoka et al. 2018).

along strike-slip faults (Birkenmajer 1991). The stratigraphic sequence of the Martel Inlet Group includes Late Cretaceous to early Miocene, calc-alkaline, predominantly volcanic rocks (basalts and andesites, with minor dacitic and rhyolitic lavas and pyroclastic rocks associated with volcaniclastic sedimentary rocks (Thomson et al. 1983, Birkenmajer 1991).

Precipitation in KGI is characterized by high annual variability, with an estimated mean of 701.3 mm during the 1968–2011 period (Kejna et al. 2013). The mean annual air temperature is approximately -1.5 °C, with the mean warmest month in January (2.4 °C) and the coldest month in June (-5.6 °C) (2012 observations by Sobota et al. (2015). Comin & Justino (2017) additionally showed an increase of 0.8–1 °C in air temperature during 1955–2010. Kejna et al. (2013) and Sobota et al. (2015) argued that the warming atmospheric trend directly interferes with the mass balance of glaciers in the KGI.

DATASETS AND METHODOLOGY

Topobathymetric data (4-meter spatial resolution)

The bathymetric data of the MI at 4-meter spatial resolution were obtained by geophysical surveys and the data comprises almost the entire underwater part of Martel inlet, except

for the sector 1.030 km away from Krak Glacier, ice-margin and new ice-free submarine areas since 2000).

Seismic and bathymetric data were multi-resolution data and were collected from three Brazilian Antarctic Expeditions (OPERANTAR): OPERANTAR XXVIII, OPERANTAR XXXI, and OPERANTAR XXXII aboard the Polar Ship Admiral Maximiano (H41), with the support of the Brazilian Antarctic Program (PROANTAR), using both Edgetech 512i sub-bottom and Kongsberg SBP 300 profilers, and a Simrad EM 302 multibeam echo sounder (frequency: 30 kHz). The sub-bottom profiler Kongsberg SBP 300 was operated with a ping-rate of 1000 ms, 2 ms pulse, and frequency envelope from 2.5 to 6.5 kHz. Magrani et al. (2015) shown the track map with the locations of the profiler lines of the sub-bottom SBP 300, Kongsberg and Edgetech 3200 surveys (Figure 2). The Simrad EM 302 multibeam, aboard the SKUA boat, was used to obtain coverage of all depths (including the <-200m) in five non-uniform spacing and parallel transects along the fjord. The areas near the Krak Glacier ice-margin (within 1,030 m of the ice-margin) and the new ice-free submarine areas (<170 m of the distance of the ice-margins) are not covered by EM302 multibeam. Bathymetry data does not cover some areas close to the ice margin (<170 m of the distance), because very shallow areas have been avoided, due to the accumulation of small icebergs. The bathymetry and topography of these sectors were covered by the General Bathymetric Chart of the Oceans (GEBCO) and REMA2 data (based on near-neighbor algorithm).

Reference Elevation Model of Antarctica (REMA) at 2-meter spatial resolution was used as the basis for interpretation of the onshore geomorphology. The REMA is a time-stamped digital surface model (DSM) of Antarctica, which includes data from WorldView-1, WorldView-2, and WorldView-3, and from a small number from GeoEye-1 images, acquired between 2009 and 2017, with most collected in 2015 and 2016, over the austral summer seasons (mostly December to March). Each DEM was vertically registered for satellite altimetry measurements (Cryosat-2 and ICESat), resulting in absolute uncertainties of

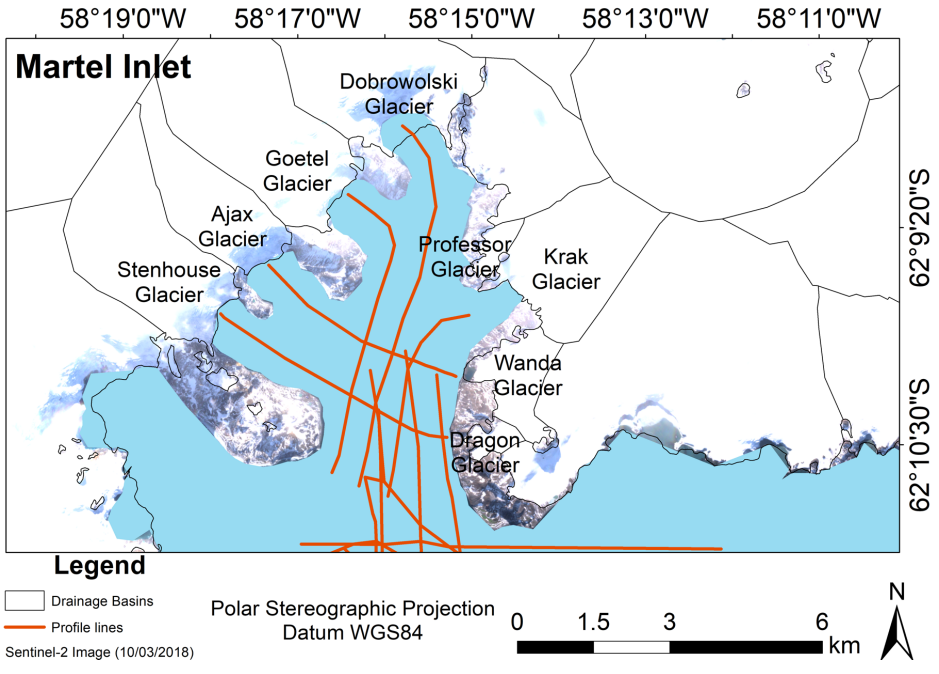

Figure 2. Track map with the locations of the profiler lines of the SBP 300, Konsberg and Edgetech 3200 sub-bottom, and Simrad 302 surveys.

less than 1 m over most of its area (Howat et al. 2019).

The REMA model-derived DEM and the bathymetric-derived product were combined using ArcGIS™ software. Inverse Distance Weighted (IDW) interpolation was applied to produce a final topobathymetric-derived product for Martel Inlet according to Ajvazi & Czimber (2019).

Geomorphometric products

Hypsometric, slope, and bathymetric profile analyses were performed. Increments of 2º were used for the classification of slopes. Geomorphometric products were processed using ArcGIS™ software.

Seismic observations

The sub-bottom profiler records by Magrani et al. (2015) (based on 2009 and 2013 field activities) and geomorphological observations based on 2007, 2010, and 2011 field activities were compiled and analyzed. The seismic or sub-bottom data was only used to extract seafloor depth and no seismic facies analysis was performed.

The subaerial (glacial and terrestrial parts of foreland), inner, middle, and outer submarine environment classification was based on depth, elevation and slope.

The submarine geomorphological mapping combined ice-marginal and subglacial landforms based on identification criteria (Table I). The dimensions, number of landforms, width, length, profile asymmetry, and spatial distance between ridges were identified to describe the landforms. The approach was based on previous work by Gehrmann & Harding (2018). The landforms were then compared to identify the differences between environments.

Chronological interpretation

For the chronological interpretation of the ice-marginal landforms, the morainal banks were grouped as follows: young (since 1970) and old (before 1970) using Sentinel-2 imagery (2018); glacial outlines (1979, 1988, 2000, and 2018) are based on GLIMS (2000), Arigony-Neto (2002), and Perondi et al. (2020).

We interpreted the ice-margin position and retreat of the glaciers based on the spatial layout of the moraines, following the approach in previous studies of glacial reconstruction (Boulton et al. 1985, Punkari 1995, Cuffey et al. 2000, Kleman et al. 2006).

RESULTS

Submarine topography and physiography of MI

The average water depth of the MI undersea sectors is 143 m, standard deviation of 111 m and maximum depth of 398 m, respectively (Table II, Figure 3). The MI bathymetry map (Figure 3 and 4) shows there are distinct geomorphometric characteristics between undersea and subaerial environments with the greatest depths the outer sector. The submarine environment has a smaller elevation range (398 m) than the subaerial elevation range of 729 m (Table II and Figure 4). The MI submarine area has an average slope of 8.7°, with the steepest slopes (>30°) in middle sector and along its outer boundary (Table III and Figure 5).

Inner Martel Inlet

The inner submarine sector ranges from 0 to 2200 m from the ice-margin. The sector has the shallowest mean depth (49 m) (Figure 4 and Table IV) of the MI submarine environment. The mean slope is 9.33°. The ice-proximal to ice-marginal and the inner/middle transition environments have steep gradients (> 30°) (Figures 5, 6).

Table I. Criteria for glacial submarine landforms identification.

Landform	Depositional Environment	Genetic process	Identification criteria	Relevance
Morainal bank	Ice-marginal. Glacier grounding line position (Streuff *et al*. 2015). They are deposited at or close to the grounding lines of water-terminating glaciers (Benn & Evans, 2010)	Formed by movement of glacigenic sediments at past glacier margin positions (Streuff *et al*. 2015). These ridges could be of glaciotectonic origin and reflect pushed-up, folded, and/or thrust sub- or proglacial environment (Streuff *et al*. 2015). Formed during a late winter readvance, followed by a summer retreat. Long-term changes in mass balance leading to major glacier advances or readvances also generate large push-moraines (Boulton 1986).	Transverse ridge (Streuff et al, 2015).	Mark the extent of glaciers (Streuff et al. 2015).
Streamlined glacial ineation	Subglacial landform is produced at the base of an active tidewater glacier (Flink *et al*. 2015, Arndt & Evans 2016).	Formed by the deposition of glacigenic deposits (Clark, 1993), and subglacial processes (Arndt & Evans 2016).	There are sedimentary elongate ridges with typical lengths of up to a few tens of kilometers, widths of a few hundred meters, and amplitudes of a few meters (Stokes & Clark 2002).	Provides direct evidence for the former presence of grounded, fast-flowing ice and can be used to infer palaeo-ice stream flow directions (Dowdeswell et al. 2006)

Table II. Hypsometric statistics for submarine and subaerial sectors in Martel Inlet.

STATISTICS OF THE HYPSOMETRIC MAP					
Sectors	**Elevation (m)**	**Minimum (m)**	**Maximum (m)**	**Mean (m)**	**Standard Deviation**
Subaerial	0/729	0	729	360	192
Submarine	0/-398	0	-398	-143	111

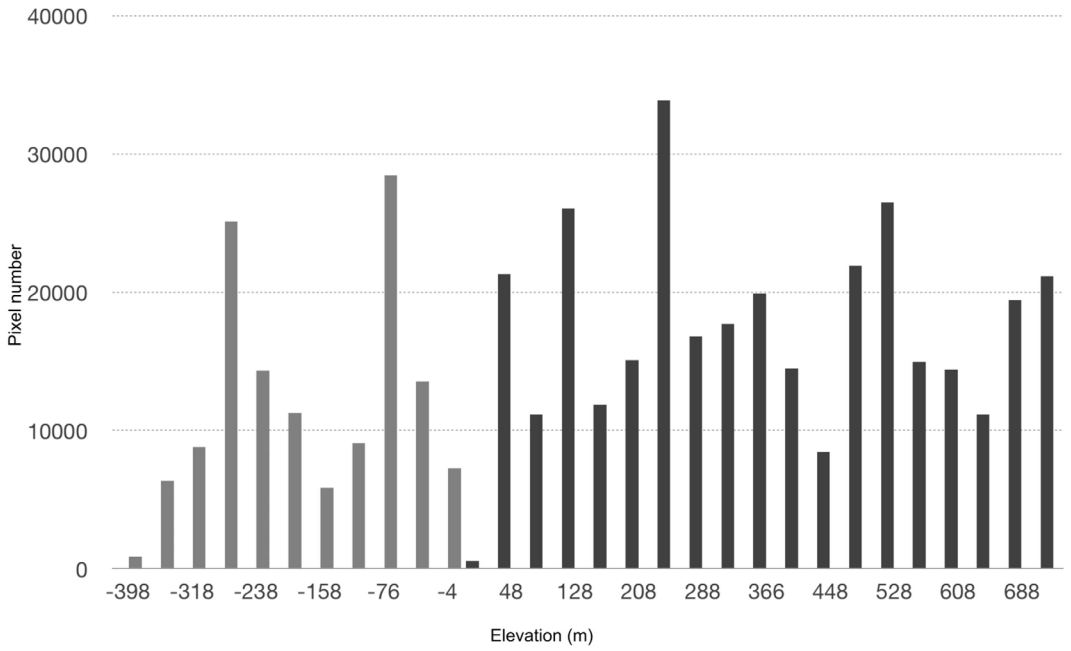

Figure 3. Distribution of subaerial and elevations.

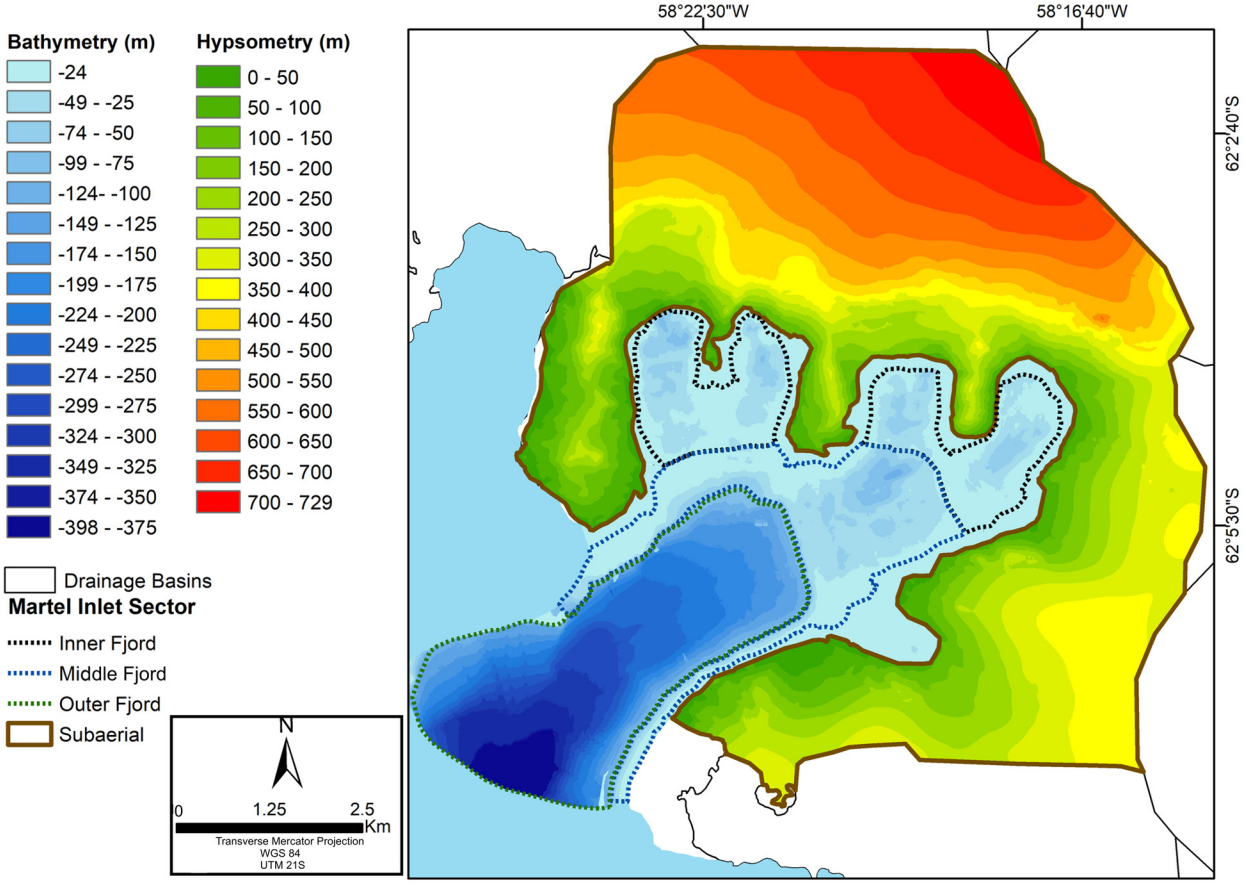

Figure 4. Bathymetric/hypsometric map of MI submarine and subaerial environments.

Table III. Absolute and relative areas, statistics of the slope classes at each sector.

SLOPE							
SUBAERIAL AREAS				SUBMARINE AREAS			
Classes (Degree)		Area (%)	Area (km²)	Classes (Degree)		Area (%)	Area (km²)
0 – 2		15.6	7.6	0 – 2		17.7	4.1
2 – 4		28.8	14	2 – 4		19.6	4.5
4 – 6		18.3	8.9	4 – 6		16.2	3.7
6 – 8		13.2	6.4	6 – 8		13.1	3
8 – 10		8	3.9	8 – 10		10.2	2.3
10 – 12		5.1	2.5	10 – 12		7.9	1.8
12 – 14		3.1	1.5	12 – 14		6	1.4
14 – 16		1.2	0.6	14 – 16		2,1	0.5
16 – 18		0	0	16 – 18		0	0
18 – 20		0	0	18 – 20		0	0
20 – 22		0	0	20 – 22		0	0
22 – 24		0	0	22 – 24		0	0
24 – 26		0	0	24 – 26		0	0
26 – 28		0	0	26 – 28		0	0
28 – 30		0.6	0.3	28 – 30		0.9	0.2
30 – 32		1	0.5	30 – 32		1.4	0.3
32 – 34		0.8	0.4	32 – 34		1	0.2
34 - 36		0.6	0.3	34 - 36		0.8	0.2
36 – 38		0.6	0.3	36 – 38		0.6	0.1
38 – 40		0.4	0.2	38 – 40		0.4	0.1
40 – 42		0.4	0.2	40 – 42		0.3	0.1
42- 44		0.4	0.2	42- 44		0.3	0.1
44- 46		0.2	0.1	44- 46		0.2	0.1
>45		1.6	0.8	>46		1.30	0.3
Minimum (Degree)	Maximum (Degree)	Mean (Degree)	Standard Deviation	Minimum (Degree)	Maximum (Degree)	Mean (Degree)	Standard Deviation
1	83	8	10	1	88	8.7	9.9

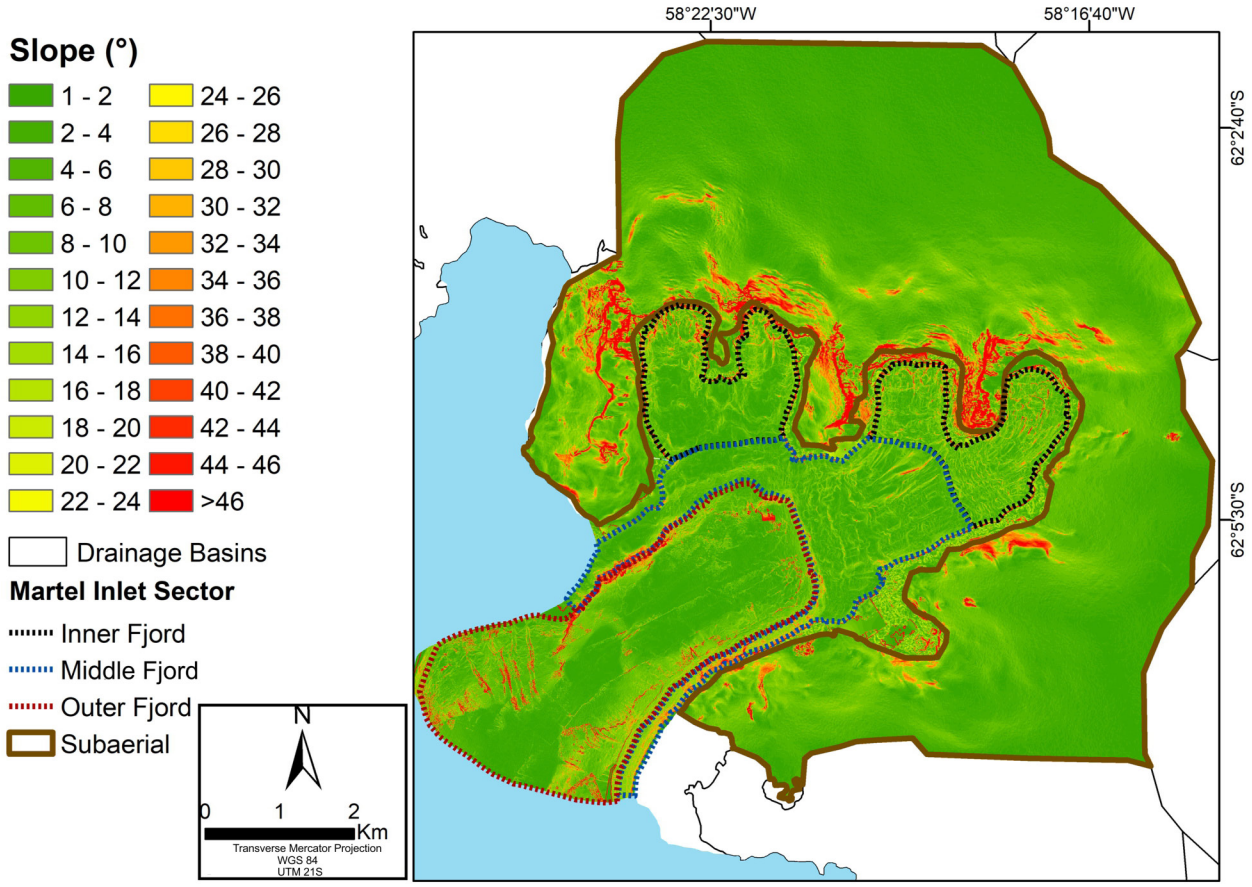

Figure 5. MI submarine and subaerial slope map.

Transverse to the fjord axis, ridges of different sizes and shapes occur in the inner part of the MI. These landforms occur at a distance of 200–2000 m from the Goetel, Ajax, Stenhouse, and Dobrowolski glacier ice margins. These landforms are interpreted as morainal banks (Figure 7). They are approximately 20 m wide, 8–35 m high, and 20–1000 m long.

The spatial distance between ridges changed from 60 m for proximal morainal banks (located at < 300 m) to 100 m for distal banks (1800 m).

The morainal banks located approximately 300 m from the Ajax-Stenhouse, Goetel, and Dobrowolski glacier fronts have approximate widths of 40, 33, and 50 m, respectively. They are characterized by sinuous and discontinuous shapes.

The two outermost morainal banks appear to be related to Ajax-Stenhouse (at 62 m water depth) and Goetel glaciers (at 70 m water depth) and are located between 2050 and 1360 m from the ice margin. They have an approximate amplitude of 40 m a width of 130 m and are characterized by a curvilinear shape.

A prominent and outermost morainal bank in the inner fjord was identified at a water depth of 34 m and 2000 m from the Dobrowolski ice margin. This feature has the steepest downstream gradient (Figures 5, 6). It has an approximate elevation of 30 m (reaching a height of 60 m at some points), a length of 675 m, and a width of 50 m, and is characterized by a curvilinear shape. This landform separates the inner and middle parts of the MI.

Table IV. Hypsometric and bathymetric statistics by MI sectors.

STATISTICS OF THE HYPSOMETRIC MAP					
Sectors	**Elevation range (m)**	**Minimum (m)**	**Maximum (m)**	**Mean (m)**	**Standard Deviation**
Subaerial	0 to 729	0	729	360	192
Submarine Inner	0 to -117	-3.33	-117	-49	20.9
Submarine Middle	0 to -188	0	-188	-55	25.5
Submarine Outer	0 to -398	0	-398	-247	77

Streamlined sedimentary glacial lineations were identified on the inner-fjord seafloor (500 – 1420 m from the ice margin). These streamlined landforms have an almost parallel orientation to the fjord axis (NE-SW direction). They are 200–300 m long and 15–30 m wide, with a mean elevation of 5 m, and are characterized by a curvilinear shape. The innermost features are smaller, aligned to N-S and NNE-SSW, and it appears that the landforms are overprinted by transverse small ridges.

Middle Martel Inlet

The middle submarine sector is located between the inner and outer sectors and has a 8,200 distance from the Dobrowolski ice margin. The mean depth was 55 m (Figures 4**,** 5, and Table IV). The mean slope was 13.2°. The slope is characterized by a gentle gradient. Variations in water depths between 80 to 60 m and steep gradients are observed near the northern and southern coasts (Figures 4, 6). There is a steeper gradient in middle/outer transition in comparison with the inner/middle transition. The Inner/middle transition has characterized by landforms groups change.

Morainal banks occur on the middle-fjord seafloor. These landforms occur transversely to the fjord axis ridges, 2200 to 4000 m from the ice margin. Morainal banks have a height of approximately 10–60 m, a length of <1000 m, and a width of 80–930 m. The crests of the highest and outermost morainal banks in this sector are at 65 m water depth.

Streamlined glacial lineations (SGL; e.g., Niessen et al. 2013) were identified with a parallel orientation to the fjord axis (NE-SW direction) and located 2,250–3,000 m from the Dobrowolski ice margin. These features have an approximate height of 10 m, a length of 400 m, and a width of 50 m, and are characterized by their straightness.

Outer Martel Inlet

The outer submarine sector is the most distal in MI and and is located 9365 m of the distance of the Dobrowolski ice margin. The mean depth was 247 m (Figure 4 and Table IV). The mean slope was 12°. The slope is characterized by a gentle gradient.

Morainal banks (Figure 7) were identified only in three sectors and are 20–30 m high, 120–520 m long, and 20 m wide. SGL were not identified in the outer-fjord seafloor (Figure 7).

MORPHOLOGY OF THE SUBAERIAL MARTEL INLET

The subaerial sector of MI (glacierized and subaerial foreland environments) includes glaciers and ice-free areas that deliver sediment and meltwater to MI. It has a mean elevation of 360 m and a maximum elevation of 729 m (with a standard deviation of 192 m) (Table IV and

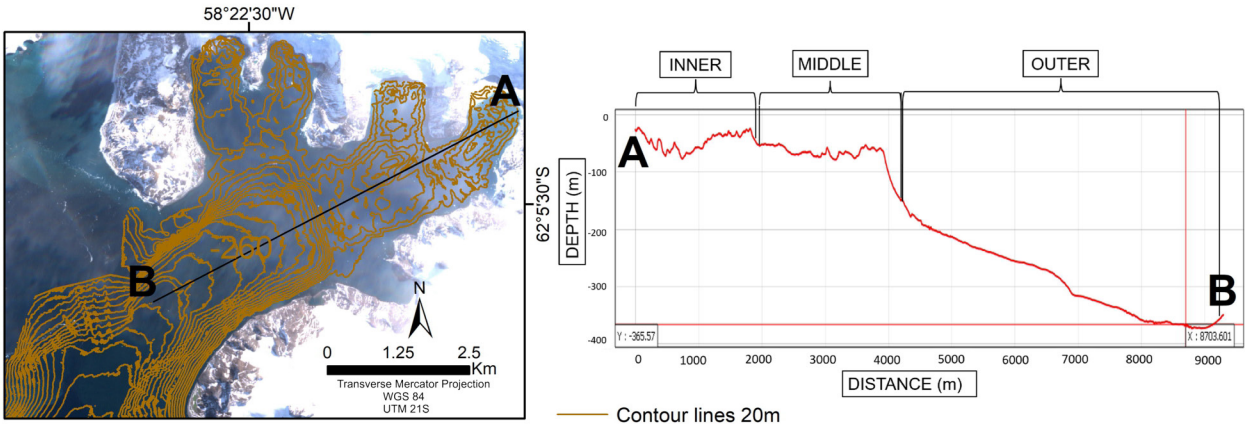

Figure 6. (1) Profile location map and contour topographic map with 20 m depth intervals; (2) Submarine topographic profile of MI. Letter A indicates the beginning of the profile and B the end of the profile.

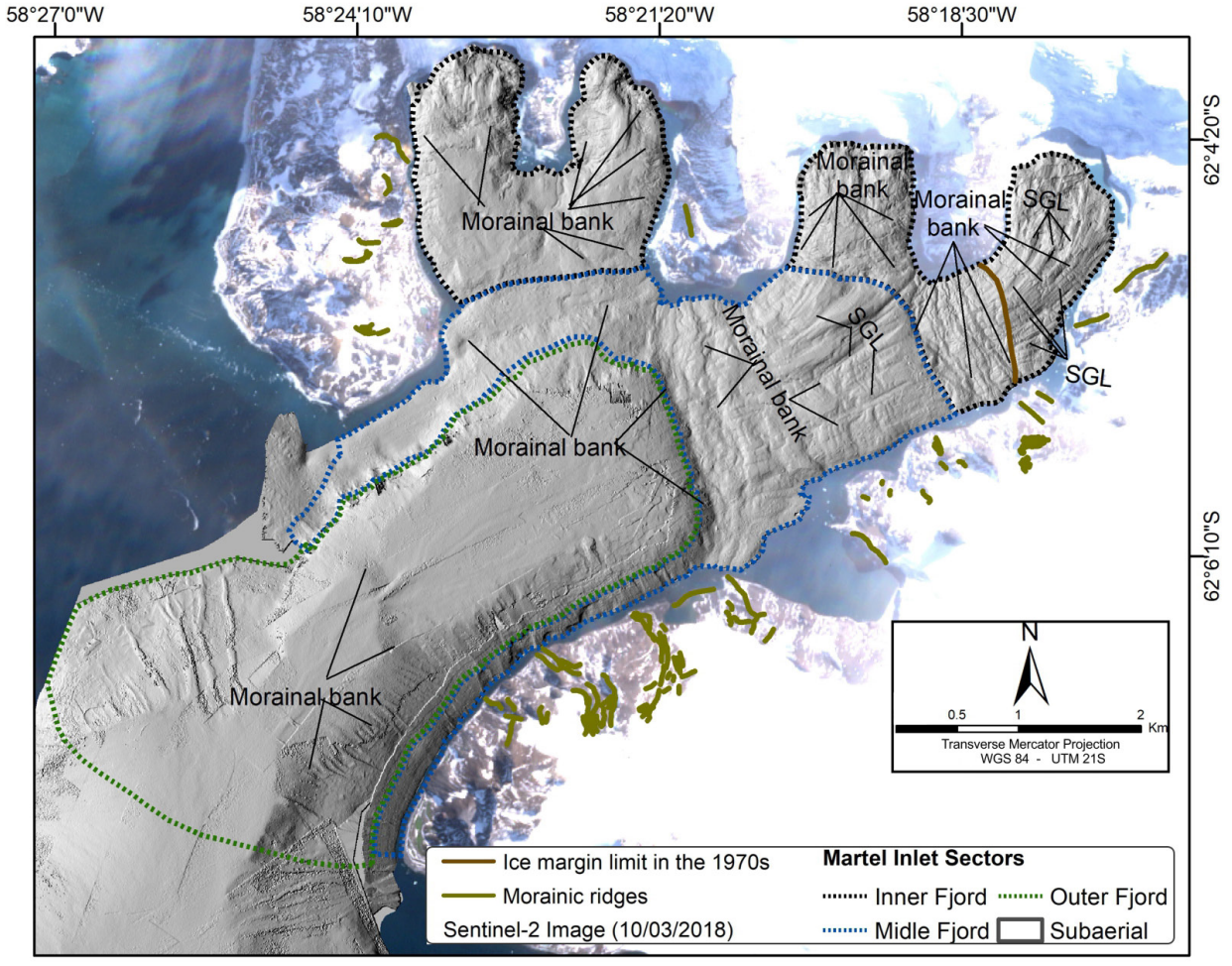

Figure 7. Streamlined glacial lineations (SGL) and ice-marginal landforms identification in shaded relief visualization of multibeam bathymetry data, overlaid on Sentinel-2 image collected in 10/03/2018.

Figure 4). 82% of the sector has a gentle slope gradient (< 10°) (Table III). The steepest areas correspond to rocky slopes and the Stenhouse, Goetel, Dobrowolski, and Ajax glaciers. The inclination directions of hillsides are mainly oriented southwest and south.

Glacial depositional features, including small recessional moraine ridges, and flutings were identified mainly in Wanda Glacier proglacial sector (Table V). Flutings are deposits 3 m long, regularly spaced and aligned parallel to the direction of ice flow

Proglacial lakes, lagoons and drainage channels are observed in Wanda Glacier foreland. Paraglacial action was identified with ravine processes, reworking of continuous morainical ridges and the presence of vegetation cover areas.

Larger transversal to ice-flow ridges are identified in Wanda, Dragon and Professor Glacier forelands and are characterized as old moraine ridges (exposed by glacier fluctuations before 1970).

DISCUSSION

Subaerial and submarine physiographic and topographic linkages and contrasts

The four sectors examined in this study have distinct morphological characteristics. The submarine physiography of the inner sector differs from the others because it displays the smallest topographic range of all sectors.

Table V. Description of glacial relief features found in the ice-free sub-aerial sector of MI.

Landform	Morphology	Glaciological significance
Lateral and frontal/recessional morainic ridges	Linear and sinuous ridges with positive relief. Ice-marginal landforms are located at the Wanda, Professor, and Dragon glaciers foreland. Most of these lateral moraines have a northeastern orientation, while the ones located on the most recent depositional margins have a northwestern orientation. A frontal moraine located at a recently ice-free area along the Wanda Glacier front has a northwestern alignment.	They were linked to stages of still stand and recession of the glacier margins. The landforms mark the outermost limit of glacier margins during still stand conditions and indicate the past glacial extent and ice-margin form.
Striated deposits	Subglacial erosional landforms formed in the direction parallel to the ice flow. These feature are identified by Rosa et al. (2013).	Subglacial meltwater action and wet thermal basal regime. Ice flow direction.
Flutings	Small-scale features streamlined and elongated in shape, with their long axes orientated in the direction of ice flow. These feature are identified by Rosa et al. (2013).	Wet basal-thermal regime of the glacier and ice flow direction.

The greatest depths in the fjord were located in the outer fjord. The outer fjord exhibits a U-shaped valley formed by ice flow from three tributary glaciers (northern and eastern sides of the MI). In the middle sector, a shallower valley, with steeper slopes, may have been filled by sediments supplied as a result of erosional glacial processes.

Most of the middle and outer-fjord are smoother, and the inner-fjord is rougher (Figure 7). The distinction between submarine sectors was made based on contrasts in depth, elevation and slope.

In addition to the presence of a more prominent morainal bank in the inner sector, there are other contrasts between the morainal banks distributed in MI (Table VI). These are related to frontal stabilizations of the Dobrowolski-Professor-Krak-Goetel glacial system and are higher amplitude in the inner than in the middle and outer-fjord sectors.

In the inner and middle MI sectors, some morainal banks crests were larger, and more spaced (distances of 100 m to 500 m between their crests) than others. There are two areas in the inner (-49 m mean depth) and middle (-55 m mean depth) sectors with push morainal banks closely spaced, compared to the other sectors of the inner, middle, and outer-fjord seafloor. In the middle and outer-fjord seafloor, morainal banks lie in an N-S orientation (Figure 7) and reflect the shape of the past glacier front.

The presence of steep submarine terrains in the middle sector (near middle and outer sector limits) provides favorable conditions for the development of gravity flows. There is a successive reworking process of the depositional features and there are links between the foreland and underwater processes. The most distal zone to the current glacial margin (Outer), before the LIA, shows reworked glacial deposits and marine sediment cover. It displays relief features in the middle sector, which are reworked, discontinuous and sparse. The inner sector, more recently exposed compared to the other sectors, displays more preserved relief features, mainly those exposed after 1970, as morainal banks. This sector receives the current input of sediments due to its proximity to the glacier front and the adjacent ice-free areas.

Table VI. Morphological characteristics of the landforms identified in the submarine environments of MI.

Morphosedimentary system	Morphology	Maximum length	Distribution in MI	Interpretation
Glacial advance and glacier stabilization	Discontinuous ridges, arranged in the N-S direction, transverse to ice flow.	632 m	Inner	Push morainal bank
	Discontinuous morainal ridges of different sizes. Further from the glacier the ridges become sparser. In the Inner environment, there are morainal banks with N-S direction and W-E.	50 - 1000 m	Inner, Middle, and Outer	Push morainal bank
Rapid ice flow	Lineations aligned in the southwest direction and transverse to the morainal banks.	200 - 500 m	Inner and Middle	Streamlined glacial lineations

In the subaerial sector, the features and their spatial arrangement also show processes of frontal glacial retraction, and sediments and water supply through melt-water channels to the glacimarine environment can be observed. To the areas exposed for a longer period (before LIA) (middle and outer sector), the influence of the glacier becomes less considerable in comparison to the marginal sector towards the ice (inner sector), and depositional landforms are less well preserved. Glacial geomorphological processes and contrasts between subaerial and undersea environments still are in course with the distance from the current glacial margin.

The modern environment and recent glacial retreat pattern

The inner submarine sector contains ice-contact, marginal, proximal, and distal (0 to 2,200 m from the actual ice margin) glacimarine environments according to the Syvitski (1993) classification. The topographic characteristics of the inner-fjord are mainly due to the presence of a variety of modern, sub-parallel morainal banks interpreted as annual push moraines.

Morainal banks in the inner sector are, in general, discontinuous and larger than those found in most parts of the middle sector. In the inner sector, a modern morainal bank is observed, older than the 1970s. Although the present study does not provide specific dating for each morainal bank, the age analysis was based on a remote sensing database.

The Ajax, Stenhouse, Dobrowolski, and Goetel glaciers have recorded recent recessional morainal banks (young, since 1979). These features show the patterns of tidewater glacier retreat caused by regional warming during the last century. The crests of the youngest morainal banks are situated at 329, 524, 525, and 1300 m from the Ajax, Stenhouse, Goetel, and Dobrowolski ice-margins, respectively. In the 1970s, glacier fronts were proximal to these morainal banks.

The Wanda, Professor, and Dragon glaciers were land-terminating during this period and their recent retreat is recorded in the subaerial environment. In subaerial areas, frontal moraines were generally curved, reflecting the shape of the glacier´s previous front.

Morainal banks in the inner sector, close to the Keller Peninsula (Figure 7), are grouped, irregular, and have been reworked by marginal ice flow. The absence of streamlined glacial lineation in this MI sector may also be a consequence of a wide layer of fine sediment covering the bottom. Glacial and marine processes transport and rework the glacimarine sediments (Dowdeswell & Scourse 1990).

Terrestrial and submarine evidence of the long-term changes in the glaciers

MI topographic profiles show that the outermost push morainal bank in the inner sector has a pronounced over-steepening on the upper proximal slope and ice-marginal depositional features of similar morphology have been related to the stages of ice-margin re-advancing in southeastern Iceland by Chandler et al. (2016).

The distal inner morainal bank recorded the last long period of stabilization for the Dobrowolski-Goetel glacial system before 1970. This feature marks the maximum length of a glacier and a long stillstand period of its terminus while grounded (e.g. Hambrey 1994, Glasser et al. 2005, Benn & Evans 2010, Streuff et al. 2015). The terrestrial extensive distal morainic ridges near the Wanda ice-margin were identified in this study. Boulton (1986) affirmed that long-term changes in mass balance, leading to major glacier advances or readvances, also produce large push moraines. Neoglacial cold events were associated with the LIA 450–250 cal yr BP (1500–1700 AD) by Simms et al. (2012), which has

been recorded by distal transverse ridges in the inner sector of the fjords in Antarctic Peninsula, as reported by Shevenell et al. (1996), Guglielmin et al. (2007), García et al. (2016) and by terrestrial morainic ridges (Hall, 2007, Dąbski et al. 2020) on Fildes Peninsula which indicate that a frontal moraine formed during the LIA.

The morainic bank in the middle sector provides records of the long-term glacial change in the region and marks a long stillstand of grounding line position during an earlier neoglacial event. These results agree with those of Wölfl et al. (2016), who showed that the outermost moraine of the Potter Cove (KGI) probably originated from a distinct stillstand of the glacier front. The authors attributed this landform to a change in climatic conditions and stabilization of the retreating Fourcade Glacier during the neoglacial period (between 2.6 and 1.6 cal kyr BP). Generally, the moraines in the inner parts of fjords developed during glacial readvances and recessional moraine ridges resulting from glacial stillstands during deglaciation (Powell 1983, Ottesen & Dowdeswell 2006, Wölfl et al. 2016).

The size and spacing of features marginal to the ice, including recessional moraines and morainal banks reflect the duration of the stabilization of the ice-margin. From the current front of the Dobrowolski Glacier to the end of the MI, there are sectors of moraine containing more continuous and less spaced ridges than in other sectors, where we can find less continuous and more spaced ridges. Moraine sectors with more continuous ridges and less spaced from each other are contiguous with the rocky outcrop alignments in the subaerial sector.

Elevated submarine rocky outcrops in these sectors may have acted as pinning points (e.g. the distal area of the inner sector in front of Dobrowolski glacier) and influenced the stabilization of the glacier margin. Once fully detached from this anchorage point, the loss of stabilizing effects of the topographic pinning points resulted in the susceptibility to a rapid glacier retreat. Smaller and more spaced annual moraines reflect higher rates of glacial ablation and retreat (Bradwell et al. 2013).

The long-term changes in calving rates and mass balance could have been the driver of the changes between the morainal bank patterns in the inner-fjord. Boulton (1986) demonstrated that a high ice velocity just exceeded by the calving rate produces closely spaced push-moraines, while a low velocity in combination with a high calving rate results in well-separated and poorly developed push-moraines.

The outer-fjord has a distinct but smooth-shaped old morainal bank that is characterized as a submarine sill. The oldest is present in the outer sector (a morainal bank with an elevation of 40 m in relation to its base) but some were also found in the middle sector (morainal bank with 100 m height) and inner sector (30 m). In addition to the exposure time, the variation in the size of the grounding line and the morainal bank is related to the thermobasal regime of the glacier and erosional and depositional rates (Powell & Alley, 2013).

Proximal to the Dobrowolski glacier front, the streamlined glacial lineations have higher ratio elongation values (e. g. 8 – 7.5) than the more distant ones (e. g. 3.8 – 5.3 values). The lineations were formed earlier than the small ridges, as indicated by the observation that the small ridges cross-cut the lineations, as identified by Wölfl et al. (2016) in Potter Cove (Maxwell Bay).

Drumlins, studied in a previous paper by Magrani et al. (2015) in MI, were identified as streamlined glacial lineations in that paper due to the radius values of such landforms in inner and middle sectors.

These lineations were not observed on the seafloor near the Wanda, Dragon, Professor, and Krak glaciers and Stenhouse-Ajax system. This may be related to the existence of conditions of slow ice-flow. However, others subglacial landforms, including striated pavements (Rosa et al. 2013) and flutings, were indicative of wet-based thermal and sliding glaciers.

Glacial lineations were also identified by Arndt (2018) in fjords in East Greenland. These features are formed under conditions of rapid glacial flow, are generally a few meters high in relation to their base (up to 50 m), and are spatially aligned to the direction of ice flow (Dowdeswell et al. 2004). Some of these elongated features initiate at knolls, such as crag-and-tails or drumlins (Arndt, 2018). Subglacial features such as these represent a wet-based thermal regime (Benn & Evans 2010). Arndt and Evans (2016) propose that streamlined glacial lineations are subglacial depositional features that involve active ice flow.

Streamlined glacial lineations are aligned N-S and NNE-SSW near the ice margin of the inner sector and change to NE-SW in the deep zones of the inner and middle sectors. These characteristics indicate that the paleo-ice flow direction changed.

Streamlined glacial lineations are larger and more widely spaced in the middle sector compared to those in the inner sector. The difference in the size of the features in each environment may be related to the erodibility of the bedrock. Thus, it appears that the glacial paleo-ice flow that united the Dobrowolski-Goetel glacial system and filled the middle sector was probably faster and thicker than current glaciers. Dowdeswell et al. (2004) noted that glacial lineations suggest a past presence of fast-flowing ice flow at the time of their formation and are conditioned by a deformable sedimentary layer at the bed.

This outermost morainal bank in the outer-fjord probably coincides with a topographic change in the basement (a higher cross-fjord elevation) and is related to a pinning point (between 100 m and 200 m water depth: Figures 6, 7). This area exhibits the steepest gradient, which is related to the Krakow fault (Figure 1C). The steep slopes, positive mass balance, ice thickness, and greater ice velocity suggest a strong glacial erosion potential in the past (Rippin et al. 2003).

The paleo-ice flow was controlled according to the orientation of the Ezcurra Fault (NE-SW). The cliffs of the valley are linked to the Ezcurra fault due to the differential erosion in MI. The Ajax-Stenhouse tributary ice-flow direction is linked to the Krakow fault-aligned N-S (Birkenmajer 1991).

The outermost morainal bank provided a stabilization for past ice-margin position at the head of the steep slope that lies seaward of it. Once detached from this topographic position the glacier was able to retreat more rapidly, with more widely spaced moraines and less continuous crests. The bathymetry and topography exert a prominent control on the tidewater glacier response to climate changes (Bianchi et al. 2020).

The hypsometric and slope values of the new DEM are in good agreement with the Admiralty Bay DEM by Rosa et al. (2014) for subaerial foreland. The advantage of the multisource and multi-resolution DEM is the automatic processing and an appropriate morphological profile that revealed the subaerial and submarine processes and glacial dynamics. The new DEM has great potential to facilitate integrated geomorphological analysis and shows actual glacier elevations.

CONCLUSIONS

The combination of DEMs and geomorphometric products for the subaerial and submarine environments in the MI showed geomorphological contrasts between the depositional environments and the pattern of glacial shrinkage since the Late Holocene. Some stabilization phases were followed by periods of more rapid retreat, as suggested by the larger spacing between morainal banks. Integrating geomorphometric and geomorphological high-resolution data from submarine and subaerial sectors of the fjord enable the understanding of the former glacier configuration and its deglaciation history.

The morainal banks formed at the last maximum advance in the LIA mark the maximum length of a glacier and a long stillstand period of its terminus while grounded.

The inner sector, close to the coastline, is quite distinct because it displays larger morainal banks, which are less reworked compared to the middle and outer regions, possibly due to the shorter duration of exposure to glacial and oceanic sedimentation. Landforms in this sector have greater amplitude when compared to other landforms, whereas in the middle sector, there is a shallower U-shaped valley, compared to downstream.

The geomorphological interpretation demonstrates a wet-based thermal regime and confluent flow direction NE-SW for past paleo-ice flow. It was possible to infer the behavior of glacial flow in the past through the presence and spacing between features, which revealed a history of deglaciation during the late Holocene.

The topography of the MI environment influenced the anchoring positions of the glacier ice margin flowing along the fjord and their ice margin stabilization in the past.

Statistical and geomorphological analysis integrated the subaerial and submarine areas and provided the distinction for each different sector. The foreland sector has links with the submarine environment through sediment input carried by the meltwater flows.

The analysis of submarine and subaerial glacial landforms will enable future studies to reconstruct fluctuations in the extent of glaciers flowing into the MI.

Acknowledgments

We acknowledge the Conselho Nacional de Desenvolvimento Científico e Tecnológico (CNPq) Project 465680/2014-3 (INCT da Criosfera), Coordenação de Aperfeiçoamento de Pessoal de Nível Superior (CAPES), Brazilian Antarctic Program (PROANTAR), Foundation of Research Support of the State of Rio Grande do Sul (FAPERGS) for financial support, and Postgraduate Program in Geography of the UFRGS.

REFERENCES

AJVAZI B & CZIMBER K. 2019. A comparative analysis of different DEM interpolation methods in GIS: case study of Rahovec, Kosovo. Geodesy Cartogr 45: 43-48.

ARIGONY-NETO J, SIMÕES JC, BREMER UF & DANI N. 2002. Perspectivas para o gerenciamento ambiental da Baía do Almirantado, ilha Rei George, Antártica. Rev Dep Geogr 15: 92-99.

ARNDT JE & EVANS J. 2016. Glacial lineations and recessional moraines on the continental shelf of NE Greenland. Geol Soc Mem 46: 263-264.

ARNDT JE. 2018. Marine geomorphological record of Ice Sheet development in East Greenland since the Last Glacial Maximum. J Quat Sci 33: 853-864.

BENN DI & EVANS DJA. 2010. Glaciers and glaciation. London: Hodder Education, 802 p.

BIANCHI TS ET AL. 2020. Fjords as Aquatic Critical Zones (ACZs). Earth Sci Rev 203: 103145.

BIRKENMAJER K. 1991. Tertiary glaciation in the South Shetland Islands, west Antarctica: evaluation of data. In: Thomson MRA et al. (Eds), Geological evolution of Antarctica. Cambridge: Cambridge University Press, p. 627-632.

BJÖRCK S, HÅKANSSON H, OLSSON, BARNEKOW L & JANSSENS J. 1993. Palaeoclimatic studies in South Shetland Islands, Antarctica, based on numerous stratigraphic variables in lake sediments. J Paleolimnol 8: 233-272.

BOULTON GS. 1986. Push-moraines and glacier-contact fans in marine and terrestrial environments. Sedimentology 33: 677-698.

BOULTON GS, SMITH GD, JONES AS & NEWSOME J. 1985. Glacial Geology and Glaciology of the Last Mid-latitude Ice Sheets. J. Geol Soc London 142: 447-474.

BRADWELL T, SIGURÐSSON O & EVEREST J. 2013. Recent, very rapid retreat of a temperate glacier in SE Iceland. Boreas 42: 959-973.

CHANDLER BM, EVANS DJA & ROBERTS DH. 2016. Characteristics of recessional moraines at a temperate glacier in SE Iceland: Insights into patterns, rates and drivers of glacier retreat. Quat Sci Rev 135: 171-205.

CLARK CD. 1993. Mega-scale glacial lineations and cross-cutting ice-flow landforms. Earth Surf Proc Land 18: 1-29.

COMIN AN & JUSTINO F. 2017. Investigação Climatológica na Península Antártica e no Arquipélago das Shetlands do Sul. Anuário IGEO 40: 74-81.

CUFFEY KM, CONWAY H, GADES AM, HALLET B, LORRAIN R, SEVERINGHAUS JP, STHEIG EJ, VAUGHN B & WHITE JWC. 2000. Entrainment at cold glacier beds. Geology 28: 351-354.

DĄBSKI M, ZMARZ A, RODZEWICZ M, KORCZAK-ABSHIRE M, KARSZNIA I, LACH K M, RACHLEWICZ G & CHWEDORZEWSKA K J. 2020. Mapping Glacier Forelands Based on UAV BVLOS Operation in Antarctica. J Remote Sens 12: 630.

DOWDESWELL JA & SCOURSE JD. 1990. On the description and modelling of glacimarine sediments and sedimentation. In: Dowdeswell JA et al. (Eds), Glacimarine Environments: Process and Sediments. Geological Society Special Publication, 53, p. 1-13.

DOWDESWELL JA, Ó COFAIGH C & PUDSEY CJ. 2004. Thickness and extent of the subglacial till layer beneath an Antarctic paleo–ice stream. Geology 32: 13-16.

DOWDESWELL JA, OTTESEN D & RISE L. 2006. Flow-switching and large-scale deposition by ice streams draining former ice sheets. Geology 34: 313-316.

DOWDESWELL JA, OTTESEN D & NOORMETS R. 2016. Submarine slides from the walls of smeerenburg fjorden, NW Svalbard. In: Dowdeswell JA et al. (Eds), Atlas of Submarine Glacial Landforms: Modern, Quaternary and Ancient. vol. 46. Geological Society, London, Memoirs, p. 105-106.

DYER KR. 1997. Estuary – A Physical Introduction. 2nd ed. Londres: John Wiley, 195p.

EVANS DJA. 2003. Glacial landsystems. Hodder–Arnold, 545 p.

FABRÉS J, CALAFAT A, CANALS M, BARCENA MA & FLORES JA. 2000. Bransfield Basin fine-grained sediments: late-Holocene sedimentary processes and Antarctic oceanographic conditions. Holocene 10: 703-718.

FLINK AE, NOORMETS R, KIRCHNER N, BENN DI, LUCKMAN A & LOVELL H. 2015. The evolution of a submarine landform record following recent and multiple surges of Tunabreen glacier, Svalbard. Quat Sci Rev 108: 37-50.

GARCÍA M, DOWDESWELL JA, NOORMETS R, HOGAN KA, EVANS J, COFAIGH CÓ & LARTER RD. 2016. Geomorphic and shallow-acoustic investigation of an Antarctic Peninsula fjord system using high-resolution ROV and shipboard geophysical observations: Ice dynamics and behaviour since the Last Glacial Maximum. Quat Sci Rev 153: 122-138.

GEHRMANN A & HARDING C. 2018. Geomorphological Mapping and Spatial Analyses of an Upper Weichselian Glacitectonic Complex Based on LiDAR Data, Jasmund Peninsula (NE Rügen). Germany Geosc 8: 208.

GLASSER NF & GHIGLIONE MC. 2009. Structural, tectonic and glaciological controls on the evolution of fjord landscapes. Geomorphology 105: 291-302.

GLASSER NF, JANSSON NK, HARRISON S & RIVERA A. 2005. Geomorphological evidence for variations of the North Patagonian Icefield during the Holocene. Geomorphology 71: 263-277.

GLIMS. 2000. Global Land Ice Measurements from Space. Available in: http://www.glims.org/ Acess in:15/01/2021.

GUGLIELMIN M, CONVEY P, MALFASI F & CANNONE N. 2007. Glacial fluctuations since the medieval warm period at Rothera point (western Antarctic Peninsula). Holocene 17: 1253-1258.

HALL BL. 2007. Late-Holocene advance of the Collins ice cap, King George island, South Shetland islands. The Holocene 17: 1253-1258.

HAMBREY M. 1994. Glacial Environments. London: UCL Press, 296 p.

HOWAT IM, PORTER C, SMITH BE, NOH MJ & MORIN P. 2019. The Reference Elevation Model of Antarctica. The Cryosphere 13: 665-674.

JOHN BS & SUGDEN DE. 1971. Raised marine features and phases of glaciation in the South Shetland Islands. Brit Antarct Surv B 24: 45-111.

KEJNA M, ARAZNY A & SOBOTA I. 2013. Climatic Change on King George Island in the Years 1948 – 2011. Pol Polar Res 34: 213-235.

KLEMAN J, HATTESTRAND C, STROEVEN AP, JANSSON KN, DE ANGELIS H & BORGSTROM I. 2006. Reconstruction of paleo-ice sheets – inversion of their glacial geomorphological record. In: Knight PG (Ed), Glacier Science and Environmental Change. Blackwell, Oxford, p. 192-198.

MAGRANI F, AYRES-NETO A & VIEIRA R. 2015. Glaciomarine sedimentation and submarine geomorphology in Admiralty Bay, South Shetland Islands, Antarctica. IEEE/OES Acoustics in Underwater Geosciences Symposium (RIO Acoustics), Rio de Janeiro, p. 1-6.

MATSUOKA K, SKOGLUND A & ROTH G. 2018. Quantarctica Dataset. Norwegian Polar Insitute.

MÄUSBACHER R. 1991. Die Jungkvartare Relief – und KlimageschichteimBereich der Fildeshalbinsel, Süd-Shetland-Inseln, Antarktis: Heidelberger. Geogr A 89: 207.

NIESSEN F ET AL. 2013. Repeated Pleistocene glaciation of the East Siberian continental margin. Nat Geosci 6: 842-846.

OTERO J, NAVARRO FJ, LAPAZARAN JJ, WELTY E, PUCZKO D & FINKELNBURG R. 2017. Modeling the controls on the front position of a tidewater glacier in Svalbard. Front 5.

OTTESEN D & DOWDESWELL JA. 2006. Assemblages of submarine landforms produced by tidewater glaciers in Svalbard. J Geophys 111.

PERONDI C, ROSA KK, PETSCH C, IDALINO FD, OLIVEIRA MAG, LORENZ JL, VIEIRA R & SIMÕES JC. 2020. Recentes alterações nas geleiras e nos sistemas paraglaciais, Antártica Marítima. Regne 6: 292-301.

POWELL RD. 1983. Glacial-marine sedimentation processes and lithofacies of temperate tidewater glaciers, Glacier Bay, Alaska. IN: Molnia BF (Ed), Glacial-marine sedimentation. Plenum Press, New York, p 185-232.

POWELL RD. 1984. Glacimarine process and inductive lithofacies modelling of ice shelf and tidewater glaciers sediments based on Quaternary examples. Mar Geol 57: 1-52.

POWELL RD & ALLEY RB. 2013. Grounding-Line Systems: Processes, Glaciological Inferences and the Stratigraphic Record, in Geology and Seismic Stratigraphy of the Antarctic Margin. Antarct Res Se 2: 169-187.

PUNKARI M. 1995. Glacial flow systems in the zone of confluence between the Scandinavian and Novaya Zemlya ice sheets. Quat Sci Rev 14: 589-603.

RIPPIN DM, BAMBER JL, SIEGERT MJ, VAUGHAN DG & CORR HFJ. 2003. Basal topography and ice flow in the Bailey/Slessor region of East Antarctica. J Geophys Res-Earth 108.

ROSA KK, VIEIRA R, MENDES JR CW, SOUZA JR & SIMÕES JC. 2013. Compilation of geomorphological map for reconstructing the deglaciation of ice-free areas in the Martel inlet, King George island, Antarctic. Rev Bras Geomorf 14: 181-187.

ROSA KK, MENDES JÚNIOR CW, VIEIRA R, DANI N & SIMÕES JC. 2014. Análise morfométrica do setor norte da baía do Almirantado, Ilha Rei George, Shetlands do Sul, Antártica. Bolet Geografia 32: 52- 61.

SHEVENELL A, DOMACK EW & KERNAN G. 1996. Record of Holocene paleoclimate change along the Antarctic Peninsula: evidence from glacial marine sediments, Lallemand Fjord Pap. Proc R Soc Tasman 130: 55-64.

SICIŃSKI J, JAŻDŻEWSKI K, BROYER CD, PRESLER P, LIGOWSKI R, NONATO EF & CAMPOS LS. 2011. Admiralty Bay benthos diversity - A census of a complex polar ecosystem. DEEP-SEA RES PT II: Topical Studies in Oceanography 58: 30-48.

SIMMS AR, MILLIKEN KT, ANDERSON JB & WELLNER JS. 2011. The marine record of deglaciation of the South Shetland Islands, Antarctica since the Last Glacial Maximum. Quat Sci Rev 30: 1583-1601.

SIMMS AR, IVINS E R, DEWITT R, KOUREMENOS P & SIMKINS LM. 2012. Timing of the most recent Neoglacial advance and retreat in the South Shetland Islands, Antarctic Peninsula: insights from raised beaches and Holocene uplift rates. Quat Sci Rev 47: 41-55.

SOBOTA I, KEJNA M & ARZANY A. 2015. Short-term Mass Changes and Retreat of the Ecology and Sphinx Glacier System, King George Island, Antarctic Peninsula. Antarct Sci 27: 500-510.

STOKES CR & CLARK CD. 2002. Ice stream shear margin moraines. Earth Surf Proc Land 27: 547-558.

STREUFF K, FORWICK M, SZCZUCINSKI W, ANDREASSEN K & Ó COFAIGH C. 2015. Submarine landform assemblages and sedimentary processes related to glacier surging in Kongsfjorden, Svalbard. ArKtos, 1.

SYVITSKI JPM, BURREL DC & SKEI JM. 1987. Fjords: Process and Products. New York: Springer-Verlag, 379 p.

SYVITSKI JPM. 1993. Glaciomarine environments in Canada: an overview. Can J Earth Sci 30: 354-371.

THOMSON MRA, PANKHURST RJ & CLARKSON PD. 1983. The Antarctic Peninsula a Late Mesozoic – Cenozoic arc (Review). In: Oliver RL et al. (Eds), Antarctic Earth Science. Camberra: Australian Academy of Science; Cambridge, p. 328-333.

WÖLFL AC, WITTENBERG N, FELDENS P, HASS HC, BETZLER C & KUHN, G. 2016. Submarine landforms related to glacier retreat in a shallow Antarctic fjord. Antarct 28: 475-486.

YOON HH, PARK B.K, KIM Y & KIM D. 2000. Glaciomarine sedimentation and its paleoceanographic implications along the fiorde margins in the South Shetland Islands, Antarctica during the last 6000 years. Palaeogeogr Palaeoclimatol Palaeoecol 157: 189-211.

How to cite
PERONDI C, ROSA KK, VIEIRA R, MAGRANI FJG, AYRES NETO A & SIMÕES JC. 2022. Geomorphology of Martel inlet, King George Island, Antarctica: a new interpretation based on multi-resolution topo-bathymetric data. An Acad Bras Cienc 94: e20210482. DOI 10.1590/0001-3765202220210482.

Manuscript received on March 30, 2021;
accepted for publication on January 22, 2022

CLEIVA PERONDI[1]
https://orcid.org/0000-0003-2202-2721

KÁTIA KELLEM DA ROSA[2]
https://orcid.org/0000-0003-0977-9658

ROSEMARY VIEIRA[3]
https://orcid.org/0000-0003-0312-2890

FABIO JOSÉ GUEDES MAGRANI[4]
https://orcid.org/0000-0002-9487-5849

ARTHUR AYRES NETO[5]
https://orcid.org/0000-0002-2982-245X

JEFFERSON C. SIMÕES[1,6]
https://orcid.org/0000-0001-5555-3401

[1]Universidade Federal do Rio Grande do Sul, Programa de Pós-graduação em Geografia, Centro Polar e Climático, Instituto de Geociências, Av. Bento Gonçalves, 9500, 91501-970 Porto Alegre, RS, Brazil

[2]Universidade Federal do Rio Grande do Sul, Centro Polar e Climático, Instituto de Geociências, Av. Bento Gonçalves, 9500, 91501-970 Porto Alegre, RS, Brazil

[3]Universidade Federal Fluminense, Instituto de Geociências, Departamento de Geografia, Av. Gal. Milton Tavares de Souza, s/n, 24210-346 Niterói, RJ, Brazil

[4]Universität Bern, Oeschger Centre for Climate Change Research & Institut für Geologie. Baltzerstrasse 1+3, 3012 Bern, Switzerland

[5]Universidade Federal Fluminense, Departamento de Geologia e Geofísica, Av. Gal. Milton Tavares de Souza, s/n, 24210-346 Niterói, RJ, Brazil

[6]University of Maine, Climate Change Institute, 168 College Ave, Orono, ME, USA

Correspondence to: **Cleiva Perondi**
E-mail: cleivaperondi@gmail.com

Author contributions

All authors analyzed the data and wrote the paper.